High-resolution angle-resolved photoemission study of USb: Dual character of $5f$ electrons

H. Kumigashira, T. Ito, A. Ashihara, Hyeong-Do Kim,* H. Aoki, T. Suzuki,† H. Yamagami, and T. Takahashi
Department of Physics, Tohoku University, Sendai 980-8578, Japan

A. Ochiai
Department of Material Science and Technology, Niigata University, Niigata 950-2181, Japan
(Received 20 August 1999)

We have performed a high-resolution angle-resolved photoemission spectroscopy (ARPES) on antiferromagnetic USb to study the electronic structure near the Fermi level. We found that USb has a metallic band structure with the fully occupied Sb $5p$ bands in contrast to semimetallic CeSb that has the partially filled Sb $5p$ bands. This suggests that the magnetic phase transition of USb is not understood within the framework of the p-f mixing model. This difference in the electronic structure between USb and CeSb is ascribed to the energy position of the respective bare f level with respect to the Sb $5p$ band. The observed fully occupied Sb $5p$ bands in USb is consistent with the band calculation based on the itinerant U $5f$ model, but different from that of the localized model. On the other hand, we found two dispersionless bands just below E_F in ARPES spectra of USb, which are well described in terms of the $5f^2$-final-state multiplet structure calculated based on the localized $5f$ model. These experimental results suggest the dual (itinerant and localized) character of $5f$ electrons that characterizes anomalous properties of USb.

I. INTRODUCTION

Uranium monopnictides (UXp;Xp=N-Bi) and monochalcogenides (UXc;Xc=S-Te) exhibit various anomalous physical properties such as the complicated magnetic phase transition with temperature and/or external magnetic field.[1,2] The observed anomalous properties have been regarded to originate in the intrinsic character of U $5f$ electrons in the compounds. It is generally accepted that $5f$ electrons are situated between ''itinerant'' $3d$ electrons and ''localized'' $4f$ electrons and thereby may have a dual character. The wide variety of physical properties of U compounds may stem from the dual character of $5f$ electrons. The ratio between the ''iteneracy'' and the ''localization'' appears to strongly depend on the counter atom in the compound, namely, the hybridization strength between the $5f$ orbital and the ligand states. In UN and US, the photoemission (PES) spectrum has a large $5f$-derived spectral weight at the Fermi level (E_F),[3,4] implying the strong itinerant nature of $5f$ electrons. In contrast, in UA's, USb, and UTe, the PES spectrum shows a clear $5f^2$-final-state multiplet structure below E_F as evidence for the localized nature of $5f$ electrons.[5]

USb with a NaCl crystal structure has been thus considered as a typical example of localized $5f$-electron materials. The large U-U spacing (~4.38 Å) in USb is well above the Hill limit[6] and, in fact, it shows an antiferromagnetic phase transition with a complicated triple-$\boldsymbol{k}$ structure[2] below T_N = 214 K.[7] The localized nature of the $5f$ electrons has been also proposed from various experiments; the relatively small electronic specific heat coefficient ($\gamma \sim 4$ mJ/mol K^2),[8] the large magnetic moment ($\mu \sim 2.85\mu_B$),[2] and observation of the crystal-field splitting by the neutron scattering.[9] From these experimental results, it has been proposed that U atoms in USb take a trivalent state and consequently USb has a semimetallic band structure with a small overlapping between the Sb $5p$ and the U $6d$ band at E_F, like semimetallic RSb (R=La and Ce) with trivalent R atoms. However, there is little consensus as for the electronic structure, in particular for the Fermi surface (FS) topology. The FS topology obtained by a recent de Haas-van Alphen (dHvA) measurement[10] is not consistent with the prediction from the band-structure calculation performed on an assumption of the well-localized $5f$ states like the $4f$ states in CeSb.[11] Further, the optical measurement suggests the existence of a relatively wide (~1 eV) U $6d$-$5f$ hybridization band at E_F, indicative of the itinerant nature of $5f$ electrons.[12]

In this paper we report a high-resolution angle-resolved photoemission (ARPES) study on antiferromagnetic USb. We found that USb has a metallic band structure with the fully occupied Sb $5p$ bands in contrast to the band-structure calculation based on the localized $5f$ model. On the other hand, the ARPES spectrum shows two U-$5f$ derived dispersionless bands just below E_F, which are ascribed to the $5f^2$ final-state multiplet structure, indicating the substantial localized nature of $5f$ electrons. Comparing the present ARPES result with that of CeSb[13,14] as well as the band-structure calculations, we discuss the nature of the U $5f$ electrons that characterize the anomalous properties of USb.

II. EXPERIMENT

Single crystals of USb were grown by the Bridgman method with a sealed tungsten crucible and a high-frequency induction furnace. High purity U ($3N$) and Sb ($5N$) metals with the respective composition ratio were used as starting materials. The obtained samples were characterized by the Debye-Scherrer method as well as the resistivity measurement. The lattice constant and residual resistivity obtained at 4.2 K are 6.210 Å and 16.7 $\mu\Omega$ cm, respectively, and are in good agreement with those of a single crystal with which dHvA signals have been observed.[10,15]

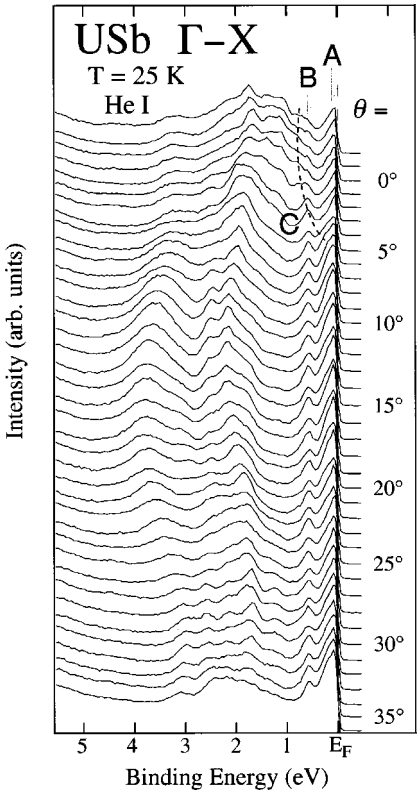

FIG. 1. High-resolution ARPES spectra of antiferromagnetic USb measured along the Γ-X direction with He I resonance line (21.2 eV) at 25 K. Polar angle (θ) referred to the surface normal is indicated.

Photoemission measurements were carried out using a home-built high-resolution angle-resolved photoemission spectrometer, which has a large hemispherical electron energy analyzer with a highly bright discharge lamp. The base pressure of the spectrometer is 2×10^{-11} Torr and the angular resolution is about $\pm1°$. The energy resolution was set at about 50 meV for quick data acquisition because of the relatively fast degradation of the sample surface. A clean mirror-like surface of the USb (001) plane was obtained by *in situ* cleaving at low temperature (25 K) just before the measurement. Since we observed degradation of the sample surface as evident by an increase of background in the spectrum, we recorded all spectra before the spectral change became detectable. The Fermi level of the sample was referred to that of gold evaporated onto the sample substrate and its accuracy is estimated to be better than 5 meV. We have performed ARPES measurements on seven different samples and confirmed the reproducibility of the data.

III. RESULTS AND DISCUSSION

A. Whole valence band region

Figure 1 shows ARPES spectra of antiferromagnetic USb measured at 25 K with the He I resonance line (21.2 eV) along the ΓX direction in the fcc (paramagnetic) Brillouin zone (Fig. 2). The polar angle (θ), referred to the surface normal of the cleaved plane, is denoted. In Fig. 1, we find two prominent dispersionless peaks (A and B) near E_F, whose energy position and intensity ratio are consistent with

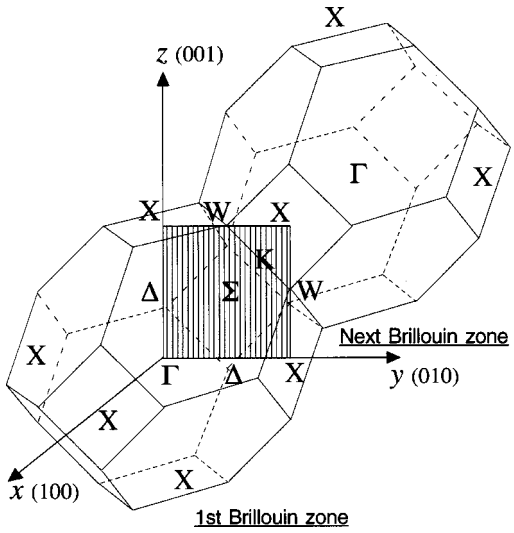

FIG. 2. Brillouin zone of fcc (paramagnetic) USb in the extended zone scheme (thin lines). ARPES measurement was performed for the ΓXXX plane.

the previous angle-integrated PES measurements.[5,16,17] Since the intensity of these two peaks is remarkably enhanced in the measurement with the He II resonance line (40.8 eV) as shown in Fig. 3, they are assigned to the U $5f$ states. The photoionization cross section of U $5f$ electrons increases drastically from the He I to the He II excitations.[18] On the other hand, the ARPES spectrum below 1 eV shows a remarkable and systematic change as a function of θ, suggesting the dispersive band structure in the high-binding energy region. In the vicinity of E_F around $\theta=0°$, we also find a small structure (marked as ''C'') which is partially covered with the prominent dispersionless two peaks (A and B).

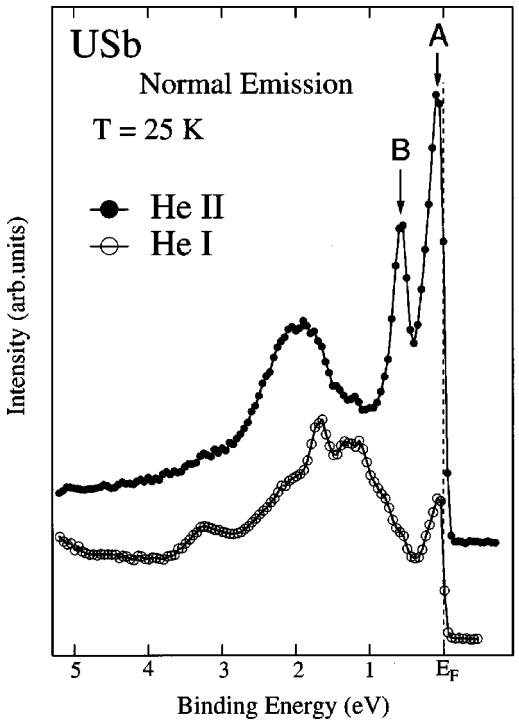

FIG. 3. Normal-emission ARPES spectra of USb measured with He I (open circle) and He II (filled circle) photons.

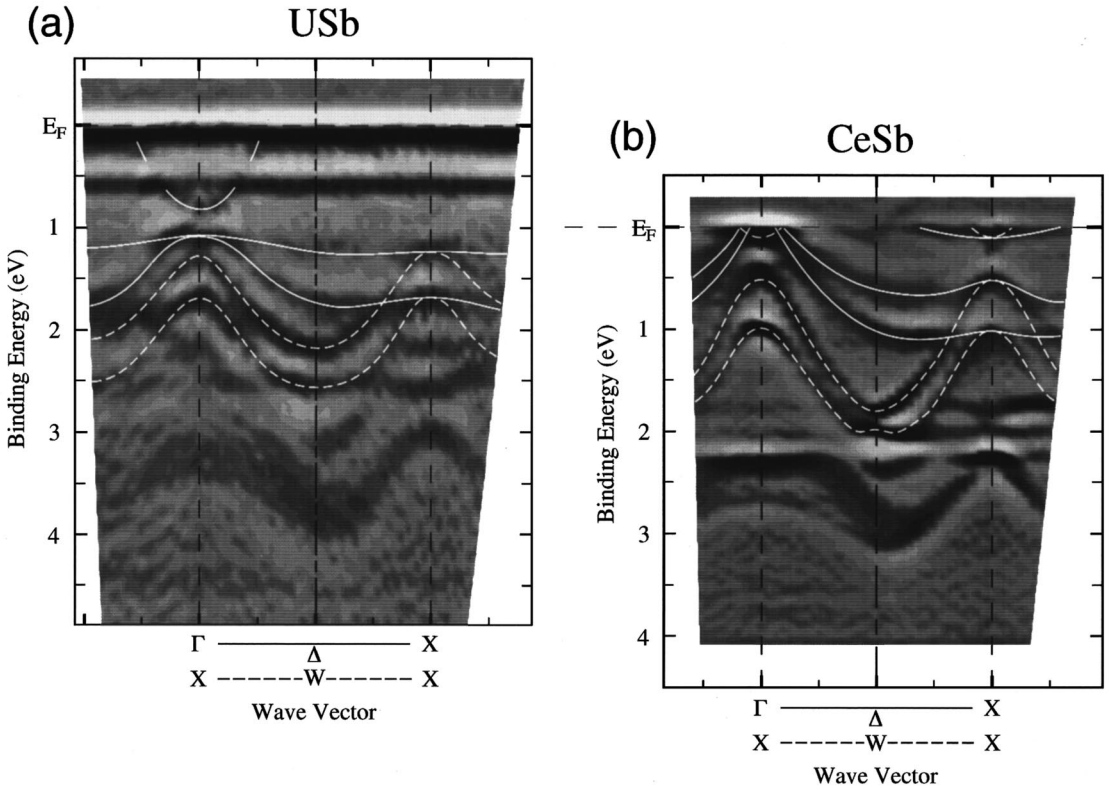

FIG. 4. (a) Experimental band structure of antiferromagnetic USb determined by the present ARPES compared with (b) paramagnetic CeSb (Refs. 13 and 14). Dark areas correspond to the energy bands. Solid- and broken-white lines are a guide to the eyes.

In order to see more clearly the dispersive feature of the bands in the ARPES spectra, we have mapped out the ''band structure'' and show the result in Fig. 4(a). The experimental band structure has been obtained by taking the second derivative of ARPES spectra after moderate smoothing and plotting the intensity in a square-root scale by gradual shading as a function of the wave vector and the binding energy,[19] dark areas correspond to the ''bands.'' This numerical procedure was employed to avoid an artificial error in the case of picking up the peak position by eyes. We set the gray-scale image so as to have the apparent bandwidth in the gray-scale image being almost equal to the full-width-at-half-maximum of the corresponding peak in Fig. 1.

It is well established that the high-symmetry lines in the Brillouin zone are likely to appear as prominent well-resolved structures in ARPES spectra.[20] This is due to the short escape depth of photoelectrons from the surface and the lack of appropriate final states in the photoexcitation process. Both cause a large broadening and uncertainty of the momentum of photoelectrons perpendicular to the surface,[21] while the momentum parallel to the surface is conserved because of the translational symmetry along the surface. This means that the ARPES spectrum mainly traces the high-symmetry lines (ΓX and XWX lines in the present case, see Fig. 2) because the density-of-states (DOS) on the high-symmetry lines is relatively large. In fact, we find in Fig. 4 that all the experimental bands are symmetric with respect to the $X(X)$ point at the Brillouin-zone boundary. This does not take place if the perpendicular component of the photoelectron momentum is conserved or not broadened. We also find in Fig. 4 that the experimental bands are categorized into two groups; one has a symmetric dispersion with respect to the W point and the other does not. It is clear that the bands belonging to the former group are ascribed to the XWX high-symmetry line while the latter to the ΓX high-symmetry line. Again, this fact gives a further experimental evidence for the substantial momentum broadening perpendicular to the surface.

B. Comparison with band-structure calculation

Next we compare the experimental band structure obtained by ARPES with the band-structure calculations performed for the two extreme cases where the U $5f$ states are treated as localized states or as bands (itinerant states). As for the localized case, the band structure of hypothetical AcSb without $5f$ electrons has been presented by Ishiguro *et al.*[10] to interpret the dHvA result. On the other hand, Weinberger and Podloucky[22] have reported the band calculation of USb where the U $5f$ states are treated as bands similar to other states such as the Sb $5p$ and U $6d$ states. But they showed the result only along the ΓX high-symmetry line. Since the band structure calculated along another high-symmetry line (XWX) parallel to ΓX is necessary to compare with the present ARPES result, we have calculated the band structure for both lines. The calculation was performed in the framework of the local-density approximation[23] with fully-relativistic linearized augmented-plane-wave (RLAPW) method.[24] The relativistic effects for all electrons were taken into account by means of the Dirac equation. In the self-consistent calculations, the valence electrons were set as $(5f)^3(6p)^6(6d)^1(7s)^2$ at the U site and $(3s)^2(5p)^3$ at the

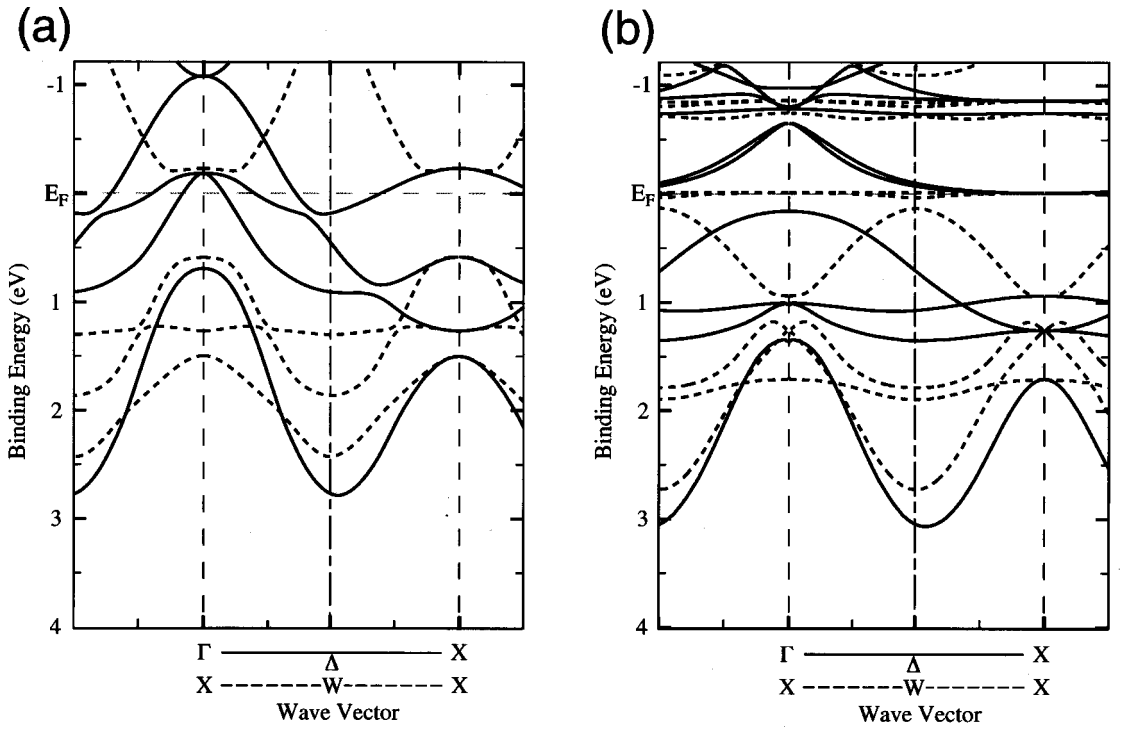

FIG. 5. Band structures of USb calculated based on (a) the localized U $5f$ model (Ref. 10) and (b) the itinerant model.

Sb site. The other electrons were treated as core electrons, which are solved under the atomiclike boundary condition. The RLAPW basis functions in the augmented-plane-wave region were expanded up to $l=8$, and the relativistic-plane-wave basis function in the interstitial region was truncated at $|\boldsymbol{k}+\boldsymbol{G}_i|<7.14(2\pi/a)$, corresponding to 387 basis functions at the Γ point. For potential convergence, 10 sampling $\boldsymbol{k}$ points in the irreducible Brillouin zone were used. The final band structure along ΓX and XWX lines were obtained from the converged potential.

Figures 5(a) and 5(b) show the band structures of USb calculated for the localized and itinerant cases, respectively. We confirmed that the obtained band structure along the ΓX line for the itinerant case [Fig. 5(b)] is almost the same as the previous report.[22] In the band-structure calculation based on the localized model [Fig. 5(a)], the top of the occupied electronic states consists mainly of the Sb $5p$ states, which split into the $5p_{3/2}$ and $5p_{1/2}$ bands by the spin-orbit interaction, while the bottom of the unoccupied states originates in the U $6dt_{2g}$ states. The calculation predicts that USb should be semimetallic due to the small overlap between the Sb $5p_{3/2}$ and U $6dt_{2g}$ bands, having two hole pockets with dominant Sb $5p_{3/2}$ character at the Γ point and one electron pocket with U $6d$ nature at the midpoint between Γ and X points. This situation is very similar to CeSb.[13,14] On the other hand, the calculation based on the itinerant model [Fig. 5(b)] predicts that USb has a metallic band structure. The Fermi level is situated in the U $6d$-$5f$ hybridized bands located at -1.0–0.9 eV, of which flat parts represent the strong U $5f$ character. The calculation shows that bands located below 1-eV binding energy are due mainly to the Sb $5p$ states. It should be noted that the Sb $5p$ bands are fully occupied in sharp contrast to the localized model.

Comparing the present ARPES result (Fig. 4) with the calculations (Fig. 5), we immediately find that the overall feature of the experimental band structure shows a better agreement with the itinerant model than the localized model. The essential factor to distinguish the two models is the location of the Sb $5p$ bands. The bands are totally occupied in the itinerant model while they are partially occupied in the localized model. In the experimental band structure (Fig. 4), we find several dispersive bands in the binding energy of 1–3 eV, which correspond to the Sb $5p$ bands in the itinerant model. In contrast, we do not find any trace of hole pockets at Γ point as predicted from the localized model. This suggests that U $5f$ electrons in USb have a substantial itinerant character and are treated as bands for understanding the electronic structure of USb. However, in contrast to a good agreement in the Sb $5p$ bands, we find that the experimental band structure near E_F is quite different from the calculation based on the itinerant model. We discuss this difference in detail later in connection with the dual character of U $5f$ electrons.

C. Comparison with CeSb

It is well established that CeSb is a semimetal with a small overlapping between the Sb $5p$ band at Γ point and the Ce $5d$ band at X point, and the $4f$ state is totally localized far away from E_F. The Ce atom thus takes a trivalent state in CeSb.[25] We show in Fig. 4 the experimental band structure of CeSb obtained by ARPES[13,14] for comparison with that of USb. It is noted that the experimental band structure of CeSb is well reproduced by the localized $4f$ model and the change of the Fermi-surface topology accompanied with the magnetic phase transition has been clearly observed by ARPES[13,14] as predicted from the p-f mixing model.[26,27] We find that the electronic structure near E_F of USb is totally different from that of CeSb. We cannot find a hole pocket at Γ point nor an electron pocket at the X point in contrast to

CeSb, but instead we observe an electronlike pocket at the $\Gamma(X)$ point in USb. Further, there are two dispersionless bands just at/below E_F in USb while they are totally missing in CeSb. On the other hand, in the higher-binding energy region, we find a very close similarity between the two compounds. According to the band-structure calculations,[26] the bands located in the high-binding energy are ascribed to the Sb $5p$ states. The dispersive Sb $5p$ bands located at 1–4 eV in USb show a very good correspondence to the bands located at E_F-3 eV in CeSb, while the Sb $5p$ bands in USb are slightly narrowed compared with those of CeSb and, what is more important, the Sb $5p$ bands are fully occupied in USb. This observation raises a serious question to the conventional explanation with the *p-f* mixing model[11] for the magnetic phase transition in USb, because the *p-f* mixing, which is the driving force in the magnetic phase transition in *semimetallic* CeSb,[26,27] cannot give any energy gain in the magnetic phase transition in USb. A different mechanism is requested to explain the magnetic properties of USb. We think that this drastic difference in the electronic structure between USb and CeSb is ascribed to the energy position of the respective bare *f* state. The occupied $4f$ state in CeSb is situated a few eV away from E_F and totally localized,[25,26] although the $4f$ state are not seen in the experimental band structure in Fig. 4(b) because of the relatively small photoionization cross section in the He I measurement. The *p-f* mixing model predicts that the Sb $5p$ band and the Ce $4f$ state overlap each other and the hybridization between the two states pushes up the Sb $5p$ band across E_F. In contrast, the occupied $5f$ state in USb is closer to E_F than the Ce $4f$ state and is consequently located above the Sb $5p$ band. The hybridization between the U $5f$ and the Sb $5p$ states rather works to push down the Sb $5p$ band toward the high-binding energy. This may be the main reason why the Sb $5p$ band in USb is narrower than that of CeSb, despite the smaller lattice constant in USb.[7,8] It is thus concluded that the difference in the energy position of the bare *f* state causes the drastic difference in the electronic structure near E_F between USb and CeSb. The U $5f$ state located very close to E_F is then expected to exhibit a strong valence fluctuation with the U $6d$ state located near E_F and thereby produce the Fermi surface different from that of CeSb.

D. Near-E_F region

In order to study the electronic structure near E_F as well as the behavior of the dispersionless U $5f$ bands in detail, we measured high-resolution ARPES spectra near E_F with a smaller energy interval and a higher signal-to-noise ratio. The results are shown in Fig. 6. We again find the two dispersionless bands (*A* and *B*) located very close to E_F and at about 0.6-eV binding energy, respectively. In the expanded energy scale in Fig. 6, we clearly find that band *A* has a shoulder at the high-binding energy and the intensity of the shoulder appears to increase at the large polar angles ($\theta > 6°$) as indicated by open circles. By further increasing the polar angle, it becomes weakened again around $\theta = 22°$. Besides the two dispersionless bands (*A* and *B*) we find a small dispersive structure around $\theta = 0°$ (band *C*), which exhibits a symmetric energy dispersion with respect to $\theta = 0°$ as shown by filled triangles. It has a bottom at ~0.8-eV binding energy

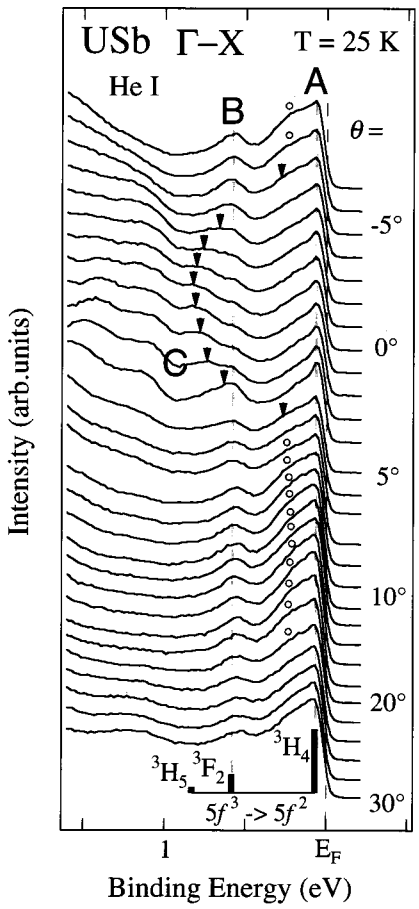

FIG. 6. High-resolution ARPES spectra near E_F of antiferromagnetic USb measured along the Γ-X direction with He I resonance line at 25 K. Polar angle referred to the surface normal is indicated. Solid vertical bars indicate the calculated U $5f^2$ final-state ($5f^3 \rightarrow 5f^2$) multiplet levels (Refs. 28 and 29).

at $\theta = 0°$ and gradually approaches E_F by increasing/decreasing the polar angle. However, it is not fully clear from the present data whether band *C* crosses E_F and enters the unoccupied states around $\theta = \pm 7°$ or it bends around $\theta = \pm 5°$ and thereafter forms a flat band just below E_F. A slight increase in the spectral intensity on the shoulder of band *A* (marked by open circles) beyond $\theta = \pm 5°$ may support the latter speculation. The next crucial issue on the electronic structure near E_F is whether the dispersionless band *A* is on or away from E_F. When we look at the slope of the ARPES spectra at E_F, we find that the midpoint of the slope is always a few meV away from E_F. This suggests that band *A* does not cross E_F at least in the ΓX (XWX) direction in the Brillouin zone. The absence of the main U $5f$ states just on E_F is consistent with the observed small electronic specific-heat coefficient.[8]

Figure 7 shows a comparison of the experimental band structure near E_F obtained by the present ARPES with the band-structure calculation based on the itinerant $5f$ model. According to the band-structure calculation, the dispersive bands located at the binding energy of more than 1 eV are ascribed to Sb $5p$ bands, while the conduction bands near E_F originate in the U $6d$-$5f$ hybridized states with a strong U $5f$ character at E_F. While the Sb $5p$ bands show a very good agreement between the experiment and the calculation

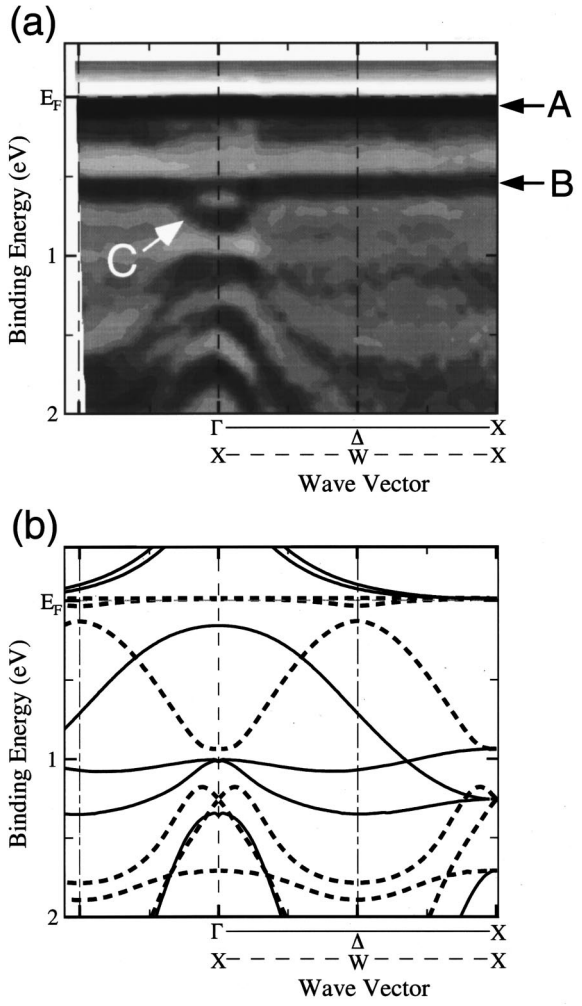

FIG. 7. (a) Experimental band structure near E_F of antiferromagnetic USb determined by the present ARPES, compared with (b) the band-structure calculation based on the itinerant $5f$ model.

as described above (see Figs. 4 and 5), the experimental band structure near E_F is substantially different from the calculation based on the itinerant $5f$ model. For example, we find in the experiment that there are two dispersionless bands (*A* and *B*) near E_F while in the calculation we find no counterpart to band *B*. As described above (Figs. 3 and 6), the two dispersionless bands have a strong U $5f$ character and band *A* is not on E_F but about 5–10 meV away from E_F in contrast with the band calculation. These results suggest the substantial localized nature of U $5f$ electrons in USb and the two dispersionless structures near E_F are assigned as the $5f^2$-final-state ($5f^3 \rightarrow 5f^2$) multiplet calculated based on the intermediate coupling scheme.[28,29] In fact, as found in Fig. 6, both the intensity ratio and the energy separation of the two peaks show a good agreement with the calculated $^3H_4$ and $^3F_2$ final states based on the $5f^3$ configuration.[28,29] In addition to these two dispersionless peaks, we find a small dispersive band (band *C*) near E_F at the $\Gamma(X)$ point in the experiment. This dispersive band may be ascribed to the U $6d$ states hybridized with the U $5f$ states by the intersite interaction, since a previous angle-integrated PES study on USb with various photon energies has suggested the existence of a substantial U $6d$ character in the DOS near E_F.[16,17] The existence of this conduction band below E_F suggests that the valency of U atoms in USb is not necessarily an integer since the U-$6d$ derived conduction band accommodates additional electrons.

A next crucial issue is whether this U-$6d$ derived band crosses E_F. According to the band calculation based on the itinerant model, bands near E_F originate in the U $6dt_{2g}$ states, which split into several bands owing to the strong U $6d$-$5f$ hybridization as shown in Fig. 5(b). Since the experimental band *C* shows an upward dispersion from $\Gamma(X)$ point [Fig. 7(a)], it might be assigned to the U $6dt_{2g}$-derived band, which is located at about 1 eV above E_F. However, this is unlikely since additional five electrons are necessary to pull down the bottom of the U $6dt_{2g}$ band below E_F. An alternative explanation is to assign band *C* to another U $6dt_{2g}$ band at the *X* point shown with the broken line in Fig. 7(b). Both the experimental and calculated bands have a bottom of the energy dispersion at about 0.8–0.9 eV at the $\Gamma(X)$ point. We find in Fig. 6 that the intensity of the shoulder of band *A* (marked by open circles) increases about midway between the $\Gamma(X)$ and $X(X)$ points. This may correspond to the flattening of the calculated lower U $6dt_{2g}$ band just below E_F around the *W* point, supporting the above assignment. However, we could not find a similar dispersive band at the equivalent $X(X)$ point as shown in Figs. 6 and 7. The reason for this discrepancy is unclear at present. A possible explanation is the transition matrix element effect and the consequent final-state broadening effect in the present ARPES experimental setup. Further ARPES studies with the varied photon energies are necessary to clarify this point.

Finally we discuss the origin for the difference in the electronic structure between USb and CeSb in connection to the difference in the character between U $5f$ and Ce $4f$ electrons. We found in this study that USb has the totally occupied Sb $5p$ bands in contrast to semimetallic CeSb. As described above, this difference originates in the energy position of the respective bare *f* level. In CeSb, the $4f$ level is situated in the middle of the Sb $5p$ band far away from E_F and gives a negligible contribution to the electronic states at E_F. This has been also confirmed by the experimental fact that overall band structure of CeSb is almost the same as that of LaSb, which has no $4f$ electrons.[30] On the other hand, in USb, the bare $5f$ level is positioned well above the Sb $5p$ band and very close to E_F, so that the *p*-*f* mixing no longer gives any energy gain for the magnetic transition. The close proximity of the U $5f$ level to E_F causes the energy instability and consequently leads to the significant valence fluctuation with the U $6d$ conduction band. As a result, the Fermi level is raised into the U $6d$-$5f$ hybridization band far from the top of the Sb $5p$ band. This difference is due to the fact that the wave function of the U $5f$ electron is spatially more delocalized than that of the Ce $4f$ electron. Indeed, the non-*f* derived part of the band structure shows a good agreement between the experiment and the calculation based on the itinerant model. In contrast, we also found that the U $5f$ derived part near E_F is well interpreted with the localized $5f$ scheme, indicating the substantial localized nature of the $5f$ electrons. This apparent self-contradiction in the ARPES spectrum suggests the dual (itinerant and localized) character of $5f$ electrons in USb. In order to obtain a better theoretical description of the electronic structure of USb, it is necessary

to incorporate the correlation effect of $5f$ electrons in the band-structure calculation or to extend the simple ionic model to the lattice model including the intersite interaction.

IV. CONCLUSION

We have performed a high-resolution angle-resolved photoemission spectroscopy on antiferromagnetic USb to investigate the electronic structure near E_F as well as the nature of U $5f$ electrons. We found that USb has a metallic band structure with the fully occupied Sb $5p$ bands in contrast to semimetallic CeSb with the partially filled Sb $5p$ bands. This requests a reinterpretation of the magnetic properties of USb so far explained based on the semimetallic band structure with the partially filled Sb $5p$ bands, because the p-f mixing can no longer give any energy gain in the magnetic transition. This difference between USb and CeSb is ascribed to the energy position of the respective bare f level with respect to the Sb $5p$ states. We found that the gross non-f derived band structure obtained by ARPES shows a good agreement with the band calculation based on the itinerant U $5f$ model. In contrast, the obtained U $5f$ derived structure near E_F is well described by the $5f^2$-final-state multiplet structure calculated based on the localized $5f$ model. The observed apparent contradiction suggests the dual character (itinerant and localized) of U $5f$ electrons in USb.

ACKNOWLEDGMENTS

The authors are grateful to Professor O. Sakai at Tohoku University for useful discussions. H.K. and H.A. thank the Japan Society for the Promotion of Science for financial support. This work was supported by a grant from the Ministry of Education, Science and Culture of Japan.

*Present address: Department of Physics, University of Seoul, Seoul 130-743, Korea.

†Present address: Institute for Solid State Physics, University of Tokyo, Kashiwa, Chiba 277-8581, Japan.

[1] J.-M. Fournier and R. Troć, in *Handbook on the Physics and Chemistry of the Actinides*, edited by A. J. Freeman and G. H. Lander (Elsevier Science, New York, 1985), Vol. 2, p. 29.

[2] G. H. Lander and P. Burlet, Physica B **215**, 7 (1995), and references therein.

[3] B. Reihl, G. Hollinger, and F. J. Himpsel, Phys. Rev. B **28**, 1490 (1983).

[4] Y. Baer, Physica **102B**, 104 (1980).

[5] B. Reihl, J. Less-Common Met. **128**, 331 (1987); B. Reihl, N. Mårtensson, and O. Vogt, J. Appl. Phys. **53**, 2008 (1982).

[6] H. H. Hill, in *Plutonium 1970 and Others Actinides*, edited by W. N. Miner (American Institute of Metallurgical Engineers, New York, 1970), p. 2.

[7] J. Schoenes, B. Frick, and O. Vogt, Phys. Rev. B **30**, 6578 (1984).

[8] H. Rudigier, H. R. Ott, and O. Vogt, Phys. Rev. B **32**, 4584 (1985).

[9] G. H. Lander, M. H. Mueller, D. M. Sparlin, and O. Vogt, Phys. Rev. B **14**, 5035 (1976); G. H. Lander and W. G. Stirling, *ibid.* **21**, 436 (1980).

[10] A. Ishiguro, H. Aoki, O. Sugie, M. Suzuki, A. Sawada, N. Sato, T. Komatsubara, A. Ochiai, T. Suzuki, K. Suzuki, M. Higuchi, and A. Hasegawa, J. Phys. Soc. Jpn. **66**, 2764 (1997).

[11] T. Kasuya, J. Phys. Soc. Jpn. **64**, 2294 (1995); T. Kasuya, *ibid.* **65**, 3394 (1996).

[12] J. Schoenes, Phys. Rep. **66**, 187 (1980).

[13] H. Kumigashira, H.-D. Kim, A. Ashihara, A. Chainani, T. Yokoya, T. Takahashi, A. Uesawa, and T. Suzuki, Phys. Rev. B **56**, 13 654 (1997).

[14] T. Takahashi, H. Kumigashira, T. Ito, A. Ashihara, H.-D. Kim, H. Aoki, A. Ochiai, and T. Suzuki, J. Electron Spectrosc. Relat. Phenom. **92**, 65 (1998).

[15] E. Hotta, A. Ochiai, Y. Suzuki, T. Shikama, K. Suzuki, Y. Haga, and T. Suzuki, J. Alloys Compd. **219**, 252 (1995).

[16] B. Reihl, N. Mårtensson, P. Heimann, D. E. Eastman, and O. Vogt, Phys. Rev. Lett. **46**, 1480 (1981).

[17] B. Reihl, N. Mårtensson, D. E. Eastman, and O. Vogt, Phys. Rev. B **24**, 406 (1981); B. Reihl, N. Mårtensson, D. E. Eastman, A. J. Arko, and O. Vogt, *ibid.* **26**, 1842 (1982).

[18] J. J. Yeh and I. Lindau, Atomic Data and Nuclear Data Table **32**, 1 (1985).

[19] F. J. Himpsel, Adv. Phys. **32**, 1 (1983).

[20] T. Grandke, L. Ley, and M. Cardona, Phys. Rev. B **18**, 3847 (1978).

[21] P. J. Feibelman and D. E. Eastman, Phys. Rev. B **10**, 4932 (1974).

[22] P. Weinberger and R. Podloucky, Phys. Rev. B **22**, 645 (1980).

[23] O. Gunnarsson and B. I. Lundqvist, Phys. Rev. B **13**, 4274 (1976).

[24] H. Yamagami, J. Phys. Soc. Jpn. **67**, 3176 (1998).

[25] M. Takeshige, O. Sakai, and T. Kasuya, J. Magn. Magn. Mater. **52**, 363 (1985).

[26] For example, T. Kasuya, Physica B **215**, 88 (1995); T. Kasuya, Y. Haga, Y.-S. Kwon, and T. Suzuki, *ibid.* **186-188**, 9 (1993), and references therein.

[27] H. Takahashi and T. Kasuya, J. Phys. C **18**, 2697 (1985).

[28] J. F. Wyart, V. Kaufman, and J. Sugar, Phys. Scr. **22**, 389 (1980).

[29] N. Beatham, P. A. Cox, A. F. Orchard, and I. P. Grant, Chem. Phys. Lett. **63**, 69 (1979).

[30] H. Kumigashira, Hyeong-Do Kim, T. Ito, A. Ashihara, T. Takahashi, T. Suzuki, M. Nishimura, O. Sakai, Y. Kaneta, and H. Harima, Phys. Rev. B **58**, 7675 (1998).